Influenza A Virus-Infected Hosts Boost an Invasive Type of *Streptococcus pyogenes* Infection in Mice

Shigefumi Okamoto,[1] Shigetada Kawabata,[1,2]* Ichiro Nakagawa,[1] Yoshinobu Okuno,[3]
Toshiyuki Goto,[4] Kouichi Sano,[4] and Shigeyuki Hamada[1]

*Department of Oral and Molecular Microbiology, Osaka University Graduate School of Dentistry, Suita-Osaka
565-0871,[1] PRESTO, Japan Science and Technology Corporation, Kawaguchi, Saitama 332-0012,[2]
Department of Virology, Osaka Prefectural Institute of Public Health, Osaka 537-0025,[3] and
Department of Microbiology, Osaka Medical College, Takatsuki-Osaka 569-8686,[4] Japan*

The apparent worldwide resurgence of invasive *Streptococcus pyogenes* infection in the last two decades remains unexplained. At present, animal models in which toxic shock-like syndrome or necrotizing fasciitis is induced after *S. pyogenes* infection are not well developed. We demonstrate here that infection with a nonlethal dose of influenza A virus 2 days before intranasal infection with a nonlethal dose of *S. pyogenes* strains led to a death rate of more than 90% in mice, 10% of which showed necrotizing fasciitis. Infection of lung alveolar epithelial cells by the influenza A virus resulted in viral hemagglutinin expression on the cell surface and promoted internalization of *S. pyogenes*. However, treatment with monoclonal antibodies to hemagglutinin markedly decreased this internalization. Our results indicate that prior infection with influenza A virus induces a lethal synergism, resulting in the induction of invasive *S. pyogenes* infection in mice.

Streptococcus pyogenes (group A streptococcus [GAS]) causes a number of diseases, including uncomplicated pharyngitis, impetigo, and acute rheumatic fever. In addition, a number of severe invasive GAS infections have been reported in North America, Europe, and Japan (2, 18, 30, 34, 36). These infections comprise a wide range of diverse diseases, including acute respiratory distress syndrome, renal failure, toxic shock-like syndrome (TSLS), sepsis, and cellulitis (2, 18, 35). Since infection can occasionally progress within hours to necrosis of an entire limb and lethal shock (2, 18, 35), GAS has become known as the "flesh-eating bug." It has been reported that many invasive GAS isolates are of the M1 or M3 serotype, which produce streptococcal pyrogenic exotoxin A (SPEA) (6, 10, 16). However, the reasons for the recent emergence or reemergence of the invasive type of GAS infection remain elusive.

GAS invades the host via the upper respiratory tract or injured skin surfaces (6); therefore, establishment of a mouse model with TSLS and necrotizing fasciitis by intranasal or subcutaneous infection with invasive GAS is important for elucidating the mechanisms responsible. Ashbaugh et al. (1) reported an invasive GAS soft tissue infection that induced necrotizing fasciitis in mice and also involved M protein, hyaluronic acid capsule, and cysteine proteases. On the other hand, a Canadian group of researchers described a case of varicella gangrenosa and GAS infection that was presented as necrotizing fasciitis of a limb (12). That study suggests that a superinfection is one of the important factors leading to an outbreak of a severe and invasive type of disease after intranasal GAS infection (12).

Statistically, the highest incidence of GAS infections occurs in winter (28). This seasonality has also been well documented in many countries, with influenza epidemics generally occurring from December to March in the northern hemisphere (3). Influenza virus infection alone is rarely lethal; however, it can promote secondary bacterial infections that are often fatal (21). Based on these findings, we examined whether nonlethal influenza A virus (IAV) infection in mice affects the outcome after superinfection with GAS in order to better understand the etiology of severe invasive GAS infection.

MATERIALS AND METHODS

Virus, bacteria, mice, and cell lines. IAV A/FM/1/47 (H1N1) (9, 32) were grown in Madin-Darby canine kidney (MDCK) cells, a canine kidney epithelial cell line (32), and then suspended in phosphate-buffered saline (PBS) before use in all subsequent studies. The GAS strains, described in Table 1, were obtained from K. Kikuchi and K. Totsuka (Tokyo Woman's Medical College, Tokyo, Japan) and T. Murai (Toho University, Tokyo, Japan) (19, 27). To detect the superantigen genes of the test strains, PCR amplification was performed as described previously (27). Formalin-fixed A/FM/1/47 were prepared at the Research Foundation for Microbial Diseases of Osaka University (Kannonji Institute, Kannonji, Japan). GAS organisms were grown for 6 h in Todd-Hewitt broth supplemented with 0.2% yeast extract (THY; Difco Laboratories, Detroit, Mich.) at 37°C. After being washed with sterile PBS, they were resuspended in PBS for mortality tests in mice. Female BALB/c mice (*H-2^d*, 8 weeks old) were purchased from SLC, Inc. (Hamamatsu, Japan). MDCK cells were grown in Eagle minimal essential medium (MEM; Sigma, St. Louis, Mo.) supplemented with 10% fetal bovine serum (Gibco-BRL, New York, N.Y.). A human alveolar epithelial cell line, A549, was grown in RPMI 1640 medium (Sigma) supplemented with 10% fetal bovine serum.

Microbial infections and counting of microorganisms in internal organs. To examine the mortality of mice infected with either IAV or GAS, or both, mice were infected intranasally with IAV (100 focus-forming units [FFU] were suspended in 25 μl of PBS) on day −2, followed by intranasal infection with GAS (10^7 CFU were suspended in 25 μl of PBS) on day 0. In some experiments, anti-hemagglutinin (HA) monoclonal antibody (MAb; C179, mouse immunoglobulin G [IgG]) (32), which inhibits the fusion of the viruses to epithelial cells

* Corresponding author. Mailing address: Department of Oral and Molecular Microbiology, Osaka University Graduate School of Dentistry, 1-8 Yamadaoka, Suita, Osaka 565-0871, Japan. Phone: 81-6-6879-2898. Fax: 81-6-6878-4755. E-mail: kawabata@dent.osaka-u.ac.jp.

TABLE 1. Mortality of mice superinfected with IAV and some invasive GAS strains

GAS strain	TSLS or non-TSLS	M type	Expression of streptococcal superantigen genes				Mortality of mice (no. dead/no. tested [%]) due to:	
			ssa	mf	speA	speC	Infection with GAS alone	Superinfection with IAV and GAS
SSI-9	TSLS	1	+	+	+	−	0/20 (0)	19/20 (95)
SSI-25	TSLS	1	+	+	+	+	0/20 (0)	16/20 (80)
SSI-1	TSLS	3	+	+	+	−	0/20 (0)	19/20 (95)
SSI-29	TSLS	3	+	+	+	−	0/20 (0)	16/20 (80)
#30	TSLS	12	−	+	+	+	0/20 (0)	18/20 (90)
SE1224	Non-TSLS	1	+	+	+	−	0/20 (0)	4/20 (20)
TW3384	Non-TSLS	3	+	+	+	−	0/20 (0)	0/20 (0)
TW3358	Non-TSLS	3	+	+	+	+	0/20 (0)	6/20 (30)
TW3346	Non-TSLS	12	+	+	+	+	0/20 (0)	2/20 (10)

(1 mg/mouse), or control mouse IgG (Jackson ImmunoResearch, West Grove, Pa.) was injected intravenously into IAV-infected mice 12 h before the GAS infection. To enumerate the number of GAS, the lungs, spleens, livers, and kidneys were dissected and homogenized in PBS. Tenfold dilutions of each suspension were plated on THY blood agar plates, and then colonies were counted after incubation overnight at 37°C. Virus numbers were assessed by a focus reduction neutralization test (33). Briefly, a suspension of MDCK cells (ca. 10^4 cells/well) was distributed into the wells of a 96-well flat-bottom plate, which was then incubated in a CO_2 incubator at 37°C to produce monolayer sheets. On the following day, 10-fold dilutions of each suspension of homogenized organ (50 μl) in MEM containing 0.2% albumin and 5 μg of trypsin (Sigma)/ml were poured into the plates containing the monolayers. Plates were then incubated for 24 h at 37°C and washed twice with PBS. After the monolayers were fixed with 99% ethanol at room temperature for 10 min and dried, focus staining was achieved by treating the cell monolayers with anti-influenza nuclear protein (NP) MAb (C43, mouse IgG; 10 μg/ml) (32), rabbit anti-mouse IgG (1:1,000), sheep anti-rabbit IgG (1:1,000), and rabbit peroxidase–anti-peroxidase (PAP) complex (1:1,000; Organon Teknika, Malvern, Pa.). Each treatment lasted 1 h and was followed by a wash with PBS. The peroxidase reaction was allowed to develop for 5 min with 0.01% H_2O_2 and 0.3 mg of 3,3-diaminobenzidine tetrahydrochloride

(Wako, Osaka, Japan) per 1 ml of PBS, and then stained cells were rinsed with H_2O and dried. Stained foci were counted by using a light microscope (Nikon, Tokyo, Japan).

Histopathology. Tissue samples were fixed in 10% (vol/vol) neutral phosphate-buffered formalin, and embedded in paraffin at 56°C. Samples were cut into 6-μm sections and stained with hematoxylin-eosin. For detection of GAS and HA-expressed cells, the sections were stained by using rabbit *S. pyogenes* SSI-1 antiserum (29) and fluorescein isothiocyanate (FITC)-conjugated anti-rabbit IgG and/or Alexa Fluor 568 (Molecular Probes, Eugene, Oreg.)-conjugated anti-HA MAb. Each section was assigned a number, which allowed an unbiased examination with a confocal microscope (Carl Zeiss, Oberkochen, Germany). For electron microscope examinations, a mixture of GAS (10^7 CFU) and IAV (10^7 FFU) was suspended in 200 μl of MEM and incubated for 2 h at 37°C in 5% CO_2. The samples were then fixed, dehydrated in ethanol, and embedded in epoxy resin (20). Ultrathin sections were made by using a Porter-Blum ultramicrotome and doubly stained with uranyl acetate and lead citrate. The sections were viewed by using an H-800 or H-7100 transmission electron microscope (Hitachi, Hitachinaka, Japan).

Assay for association and/or invasion of GAS. IAV (2×10^4 FFU in MDCK cells and 2×10^6 FFU in A549 cells) were used to inoculate semiconfluent cell
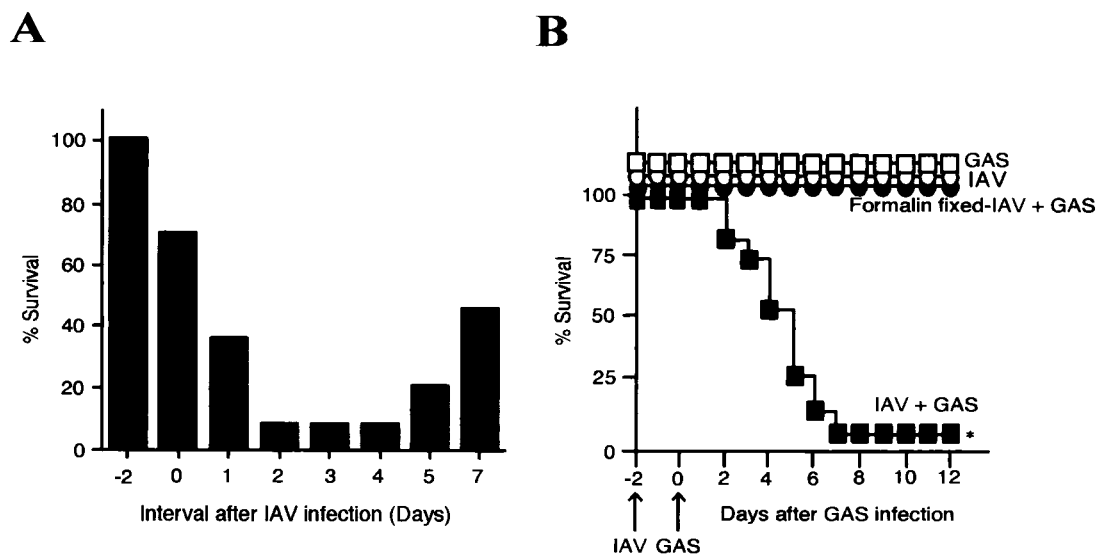

FIG. 1. Lethality of mice superinfected with IAV and GAS. (A) Groups of mice (n = 20) were infected with IAV strain A/FM/1/47 (100 FFU suspended in 25 μl of PBS) on day 0 and GAS strain SSI-1 (10^7 CFU suspended in 25 μl of PBS) on days −2, 0, 1, 2, 3, 4, 5, and 7. The rate of survival 14 days after GAS infection was then calculated. (B) A total of 108 mice were divided into four groups of 27 mice each. The first 27 mice (□) were injected with 25 μl of PBS on day −2, followed by intranasal infection with GAS strain SSI-1 (10^7 CFU suspended in 25 μl of PBS) on day 0. Another 27 mice (○) were infected intranasally with IAV strain A/FM/1/47 (100 FFU suspended in 25 μl of PBS) on day −2, followed by intranasal injection with 25 μl of PBS on day 0. Another 27 mice (■) were superinfected intranasally with IAV on day −2 and GAS on day 0. The remaining 27 mice (●) were superinfected intranasally with formalin-fixed IAV on day −2 and GAS on day 0. The mortality of the mice was assessed 12 days after the GAS infection. ∗, P < 0.001 (compared to the □, ○, and ● data).

monolayers (10^5 cells) in 24-well culture plates with 200 μl of MEM (pH 6.0), containing 0.2% bovine serum albumin (fraction V; Sigma) and 1 μg of trypsin (acetylated; Sigma)/ml for 30 min at 37°C in 5% CO_2. After the medium was aspirated, 1 ml of conditioned medium was poured into the wells, which were then incubated for 17 h at 37°C in 5% CO_2. After the cells were washed, fresh GAS organisms (10^6 CFU) were suspended in 200 μl of conditioned medium and used to inoculate the cell monolayer for 2 h at 37°C in 5% CO_2. After the unattached bacteria were washed out with PBS, MDCK cells were disrupted, serially diluted by addition of sterile distilled water, and plated on THY agar plates to determine the total number of GAS organisms associated with the epithelial cells. For invasion assays, superinfections of GAS (10^6 CFU/200 μl of conditioned medium) were achieved by inoculating cell monolayers for 2 h at 37°C in 5% CO_2, after which unattached bacteria were removed by a wash with 1 ml of PBS. The GAS associated with the cell surfaces was killed by treatment with gentamicin (100 μg/ml) and penicillin (10 U/ml) for 1 h. Cell monolayers were then washed, disrupted with sterile distilled water, serially diluted in water, and plated on THY agar plates to determine the number of internalized GAS bacteria. In some experiments, 200 μl of anti-HA MAb (1 mg/ml), suspended in the conditioned medium, was added to the plates and then incubated for 1 h at 37°C in 5% CO_2 before GAS infection.

Cytokine assays. Bronchoalveolar lavage (BAL) fluid was obtained by washing the incised trachea with 0.7 ml of cold PBS containing 0.1% EDTA three times (7). The BAL fluid was centrifuged at $3,000 \times g$ for 10 min, and the supernatants were stored at −70°C until use. The measurement of cytokines, including interleukin-1β (IL-1β), IL-6, and tumor necrosis factor alpha (TNF-α), was performed with the BAL fluid samples by using an enzyme-linked immunosorbent assay as described previously (31).

Statistical evaluations. The Mantel-Cox test was performed with StatView software (SAS Institute Inc., Cary, N.C.) to determine significant differences in the mortality experiments. To analyze the data from other experiments, a nonparametric Mann-Whitney U test was done. All conclusions were based on a significance level (P) of <0.05.

RESULTS

Enhanced lethality of mice infected with IAV prior to GAS. We infected groups of mice intranasally with IAV, followed by superinfection with GAS intranasally. Mice were killed at the highest mortality when the intervals between IAV and GAS infections were 2 to 4 days (Fig. 1A). IAV- or GAS-infected mice and formalin-fixed IAV- and GAS-superinfected mice all survived for at least 10 days after infection. Ninety-three percent of mice infected intranasally with GAS after IAV infection died within 7 days of the GAS infection (Fig. 1B). Superinfection with IAV and other TSLS-GAS strains also led to more than 80% of mice to death within 2 weeks of the GAS infection (Table 1). Dissection of the dead superinfected mice revealed marked swelling of the lungs (Fig. 2A); however, such changes were not found in the lungs of mice infected with either GAS or IAV alone or in the uninfected controls (Fig. 2A). Histopathologically, the pulmonary alveoli from mice infected with both GAS and IAV were filled with an exudate containing leukocytes, erythrocytes, and bacteria; this finding was in contrast to mice infected with either GAS or IAV (Fig. 2B).

Appearance of necrotizing fasciitis in mice after superinfection. We assessed the mortality of mice by the superinfection for three experiments and found that 7 of 67 mice that died after superinfection exhibited necrotizing fasciitis in the femoral or forelimb region (Table 2 and Fig. 3A and B). These necrotic lesions appeared within the 24 h period preceding death. We also found clusters of GAS bacteria in different parts of the muscles, connective tissues, and blood vessels of necrotized tissues (Fig. 3C), which were confirmed by staining with specific rabbit anti-GAS polyclonal antibodies (Fig. 3C). The abdominal cavities of the killed mice were filled with pus,
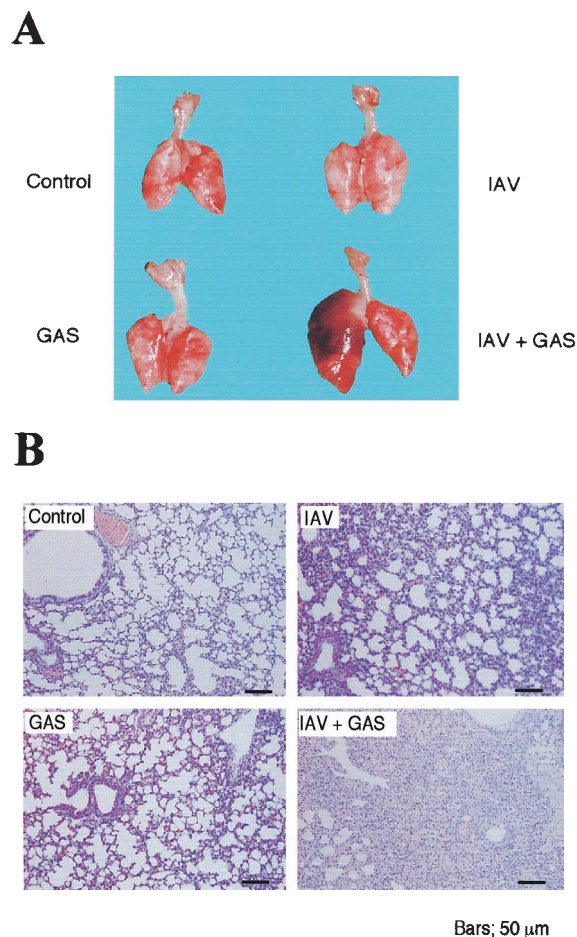
Bars; 50 μm

FIG. 2. Histopathological changes in lungs of mice infected with GAS and/or IAV. Macrography (A) and micrography (B) of the lungs assessed 4 days after the GAS infection.

and the structural integrity of the internal organs was severely damaged (Fig. 3D). The number of GAS organisms in the liver, spleen, kidneys, and blood of the dead mice with necrotizing fasciitis was 50 to 200 times higher than that found in superinfected mice that had died without exhibiting necrotizing fasciitis (Fig. 3E).

Distribution of the spread of GAS and IAV. GAS bacteria were not detected in any internal organs of mice infected with GAS alone. In contrast, a large number of GAS organisms were detected in the lungs of superinfected mice 24 h after the GAS infection (Fig. 4A). The number of GAS increased there-

TABLE 2. Number of dead mice with necrotizing faciitis

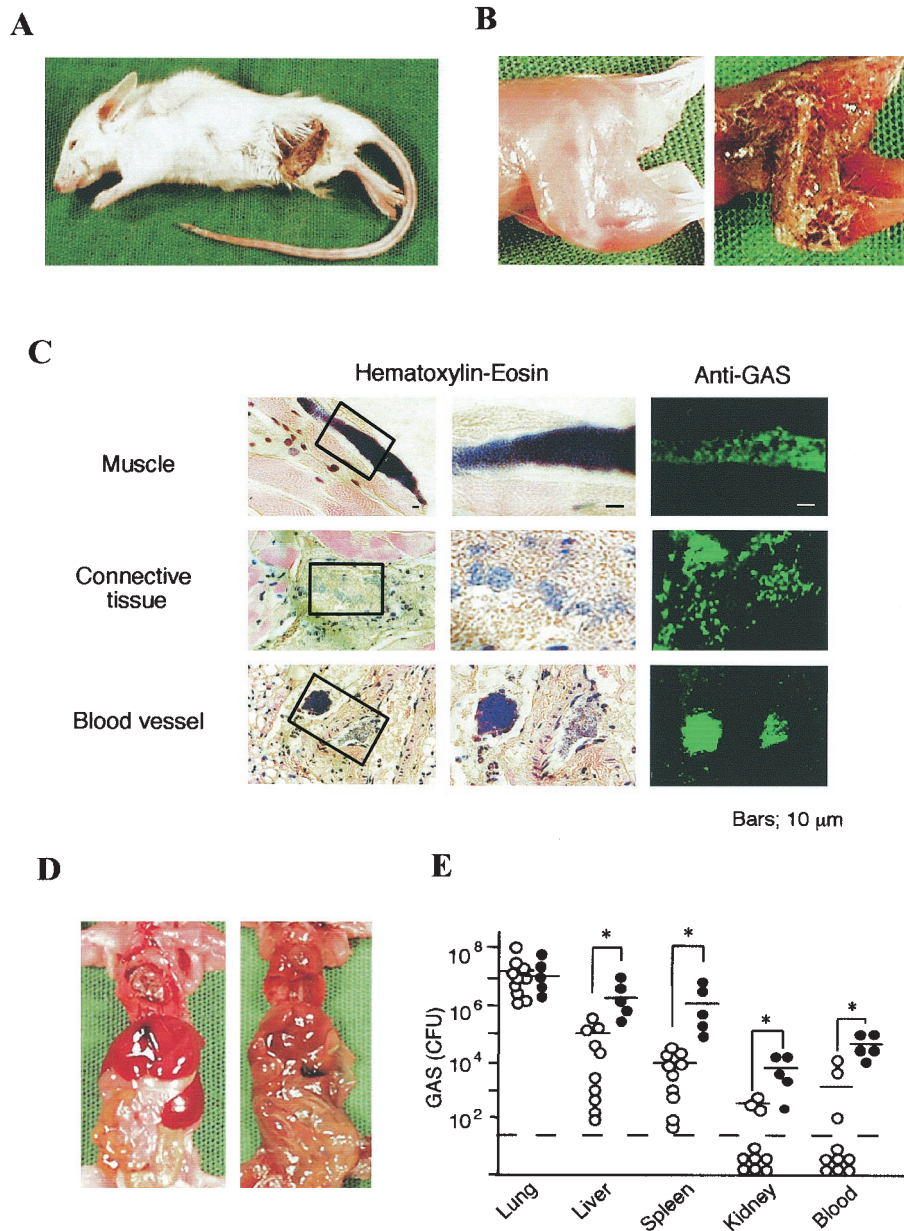| Expt	No. of mice		
	Tested	Dead	Dead with NF[a]
1	27	25	3
2	20	19	1
3	20	17	3
Total	67	61	7

[a] NF, necrotizing fasciitis.

FIG. 3. Gross pathology of mice with necrotizing fasciitis. (A) Mouse superinfected intranasally with IAV and GAS that died 4 days after the GAS infection. A characteristic appearance of skin necrosis and necrotizing fasciitis can be seen. (B) Hind leg of a noninfected mouse (left) and the dead mouse shown in panel A (right). (C) Histopathology of the necrotic lesion from the mouse shown in panel A. Staining with hematoxylin-eosin (left and middle columns) and immunostaining with rabbit antiserum against GAS and FITC-conjugated anti-rabbit IgG (right column) was done. (D) Internal organs of a noninfected mouse (left) and the superinfected mouse (right). (E) Number of GAS organisms recovered from the lungs, liver, spleen, kidneys, and blood (100 μl) from each dead mouse with ($\bullet$; $n = 5$) or without ($\bigcirc$; $n = 10$) necrotizing fasciitis. Open circles under the broken line indicate that any bacteria were not detectable. $-$, median values; $\ast$, $P < 0.05$.

after and up to 72 h after the GAS infection, after which time GAS had spread deep into the liver, spleen, and kidneys (Fig. 4A). We also detected IAV in the lungs of mice infected either with IAV alone or with IAV and GAS (Fig. 4B). The number of IAV in superinfected mice was significantly higher than that in mice infected with IAV alone in the early phase of the infection. However, the number of IAV was decreased to a similar level in these two groups of mice after 72 h (Fig. 4B). These results suggest that the superinfected mice died from

septic attacks due to increasing number of GAS in different organs and the circulation.

Effect of IAV HA on internalization of GAS into epithelial cells. We measured the number of GAS associated with IAV-infected or noninfected MDCK and A549 cells. The number of GAS associated with IAV-infected cells was more than 10 times higher than that found in the noninfected cells (Fig. 5A and B). It is known that IAV-infected cells express HA from the IAV (4, 5, 13, 26); therefore, we hypothesized that HA
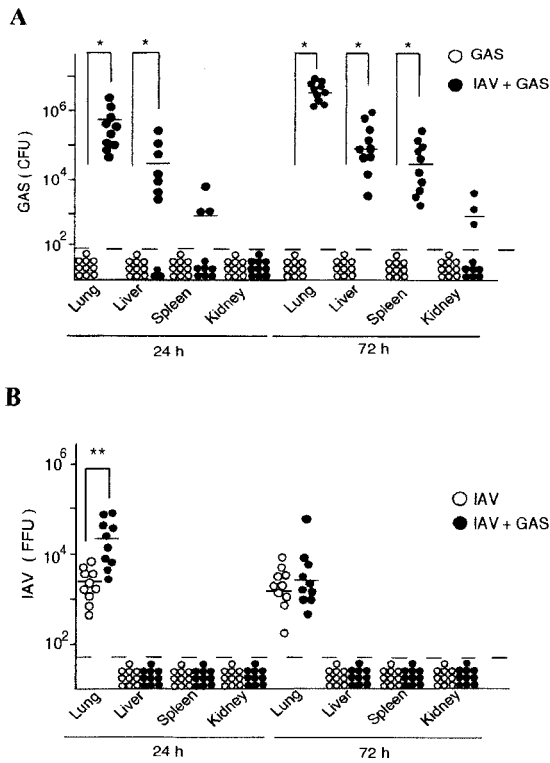
A

B

FIG. 4. Number of microbes in the organs of mice. (A) Twenty mice were divided into two groups. Ten mice (○) were infected intranasally with GAS on day 0, and ten mice (●) were superinfected intranasally with IAV on day −2 and with GAS on day 0. The number of GAS organisms in the internal organs of each group was assessed 24 and 72 h after the GAS infection. (B) Twenty mice were divided into two groups. Ten mice (○) were infected intranasally with IAV on day −2, and ten mice (●) were superinfected intranasally with IAV on day −2 and GAS on day 0. The number of IAV particles was assessed 24 and 72 h after the GAS infection. The open and closed circles under the broken line indicate that no GAS or IAV was detectable. −, median values; *, $P < 0.01$; **, $P < 0.05$.

expressed after IAV infection could result in an increased association and/or invasion of GAS in the MDCK cells. Interestingly, we found that a considerable number of cells prepared from the superinfected mice clearly expressed HA. In addition, pretreatment of IAV-infected cells with fusion inhibiting anti-HA MAb suppressed the association and/or invasion of GAS (Fig. 5A and B). We also attempted an electron microscopic observation for the binding of GAS to the IAV-infected MDCK cells, which expressed HA. As shown in Fig. 5C, the GAS bacteria were bound to IAV particles on the epithelial cell surfaces.

We examined the distribution and localization of GAS after the expression of HA on alveolar epithelial cells of the superinfected mice. Fluorescence microscopy revealed the existence of GAS organisms in alveolar epithelial cells of the superinfected mice, whereas none were detected in the cells from mice infected with GAS alone (left and center panels of Fig. 6). Furthermore, an intravenous administration of anti-HA MAb into the superinfected mice 12 h before GAS infection markedly suppressed the persistence of GAS along the epithelial cells (right panels of Fig. 6). These results suggest that IAV
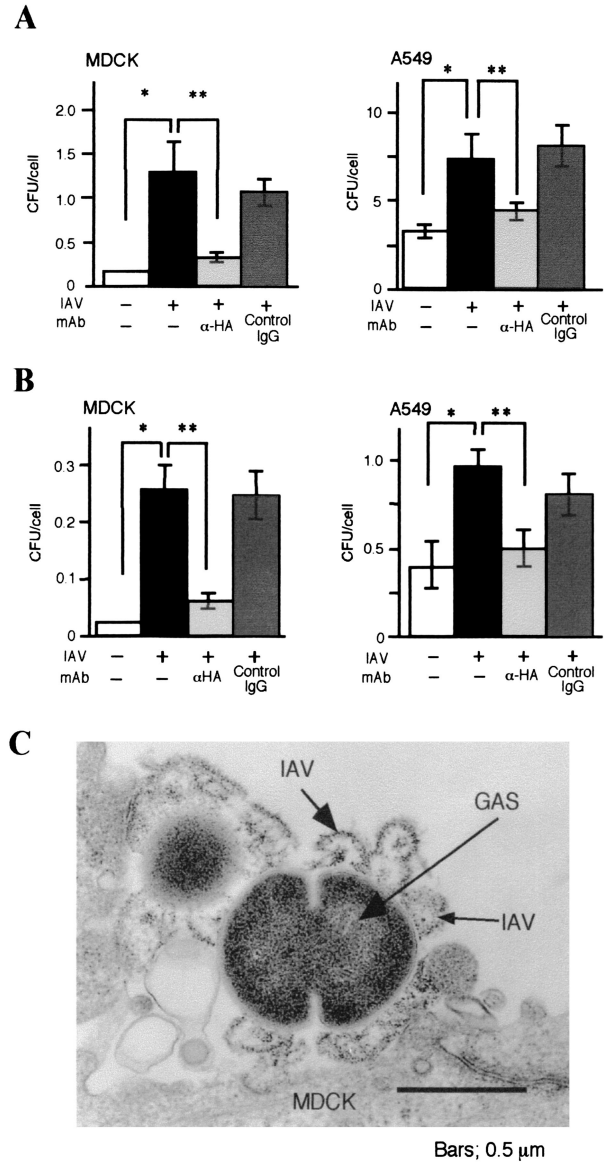
A

B

C

Bars; 0.5 μm

FIG. 5. Internalization of GAS into IAV-infected cultured cells and inhibition by anti-HA MAb. MDCK and A549 cells were infected with IAV, followed by treatment with anti-HA MAb (light gray), or the control mouse IgG (dark gray). After two washes, cultured cells were infected with 10^6 CFU of GAS for 2 h. (A) Number of GAS organisms associated with one MDCK or A549 cell. (B) Number of invaded GAS organisms in one MDCK or A549 cell. Noninfected and superinfected groups appear as open and closed bars, respectively. The data shown are representative results from five separate experiments. *, $P < 0.01$ (compared to the open bar data); **, $P < 0.01$ (compared to the data in the light gray bar). (C) Electron micrograph of GAS adhering to IAV on MDCK cell surface. MDCK cells were infected with IAV, followed by the treatment with GAS for 2 h.

infection may play a role in the enhanced internalization of GAS into alveolar epithelial cells, resulting in the emergence of sepsis by GAS and invasive GAS diseases.

Inhibition of the outbreak of invasive GAS infections by anti-HA MAb. To clarify the role of the expression of HA in vivo, we injected mice intravenously with an anti-HA MAb 2 days after the IAV infection. After 12 h, mice were infected
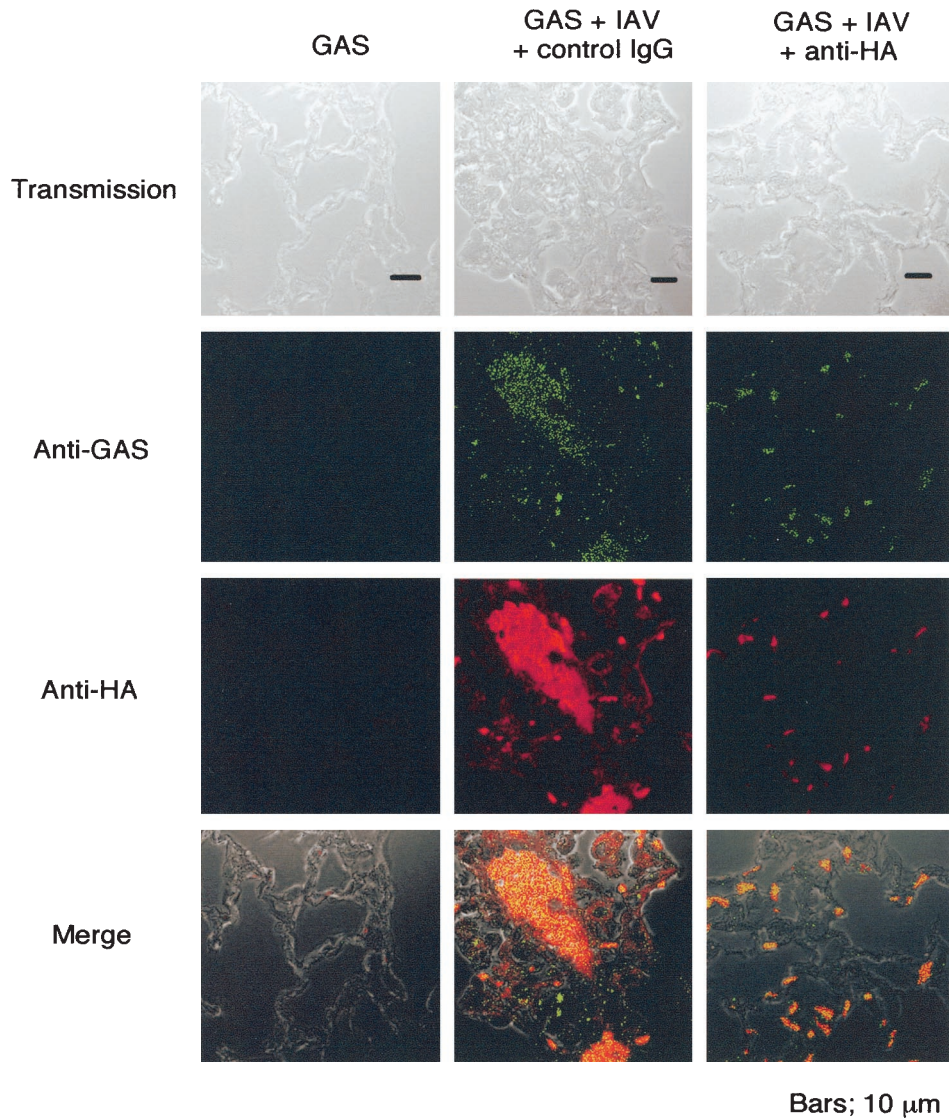
Bars; 10 μm

FIG. 6. Internalization of GAS to IAV-infected alveolar epithelial cells and its inhibition by anti-HA MAb. Mice were infected with GAS alone or superinfected with GAS and IAV as described for Fig. 2. Some superinfected mice were treated intravenously with anti-HA MAb 12 h before GAS infection. Lung sections were stained with Alexa Fluor 568-conjugated anti-HA MAb or polyclonal rabbit antibody against GAS and FITC-conjugated anti-rabbit IgG.

with GAS. Administering anti-HA MAb intravenously into the superinfected mice clearly suppressed edematous swelling and injury of the lung (Fig. 7A and B). We also found that treatment of the superinfected mice with anti-HA MAb decreased the number of GAS organisms not only in the lungs but also in the liver, spleen, and kidneys (Fig. 7C). More than 70% of the superinfected mice survived after treatment with the anti-HA MAb, whereas more than 80% of the mice died within 7 days of superinfection without the administration of anti-HA MAb (Fig. 7D).

Since HA interacts with sialic acid (4, 5, 13, 26), we determined the amount of sialic acid of the GAS organisms. Only trace amounts of sialic acid were detected in the whole cells of all GAS strains examined, and there was no significant difference in the sialic acid contents between invasive and noninva-

sive GAS strains. Furthermore, pretreatment of GAS with sialidase did not suppress the adhesion/invasion of GAS to the IAV-infected epithelial cells (data not shown).

TNF-α and IL-6 levels after IAV and GAS infections. We assessed cytokine production in BAL fluid from the superinfected, monoinfected, and noninfected mice. As shown in Fig. 8, both TNF-α and IL-6 levels in BAL fluid from superinfected mice were clearly higher than those in the other groups of mice; however, IL-1β production was not significantly increased by the superinfection.

DISCUSSION

We have demonstrated here that intranasal infection with sublethal doses of IAV into mice resulted in lethal infection
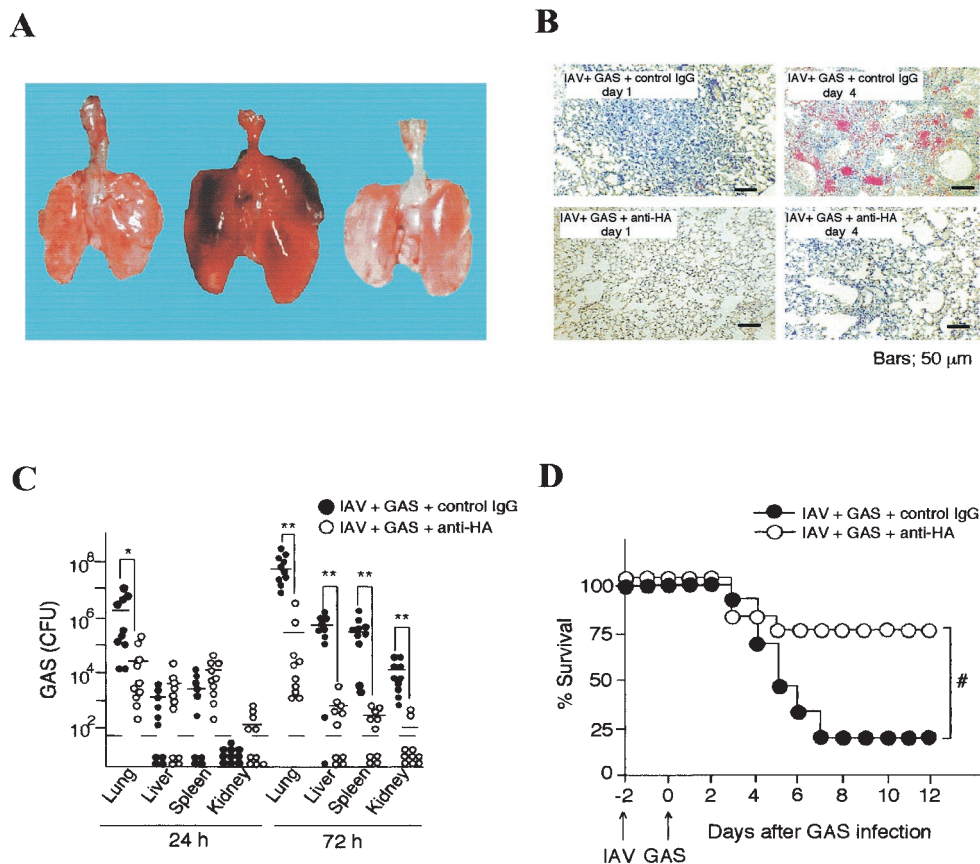
FIG. 7. Passive immunity of mice from anti-HA MAb. (A) Macrography of lungs of a normal mouse (left), an IAV-GAS-infected mouse (center), and an IAV-GAS-infected and anti-HA MAb-treated mouse (right) harvested 4 days after GAS infection as described in Materials and Methods. (B) Micrography of lungs from IAV-GAS-superinfected and control mouse IgG-treated mice (upper panels) and IAV-GAS-superinfected and anti-HA MAb-treated mice (lower panels). (C) A total of 40 mice were infected intranasally with GAS and IAV as described for Fig. 2. Twenty mice (○) were treated intravenously with anti-HA MAb, and twenty mice (●) were given normal mouse IgG. Ten mice from each group were killed 24 and 72 h after GAS infection, and the numbers of GAS organisms in the lungs, liver, spleen, and kidneys were determined. Circles under the broken lines indicate that GAS was not detectable. −; median values. *, $P < 0.05$ (compared to ● data); **, $P < 0.01$ (compared to ● data). (D) Survival of mice superinfected with GAS and IAV by intravenous administration of anti-HA MAb. Sixty mice were divided into two groups. Thirty of the mice (●) were infected with IAV on day −2 and then treated with normal mouse IgG (1 mg/mouse, given intravenously) on day −0.5, followed by intranasal infection with GAS on day 0. The remaining 30 mice (○) were infected with IAV on day −2 and then treated intravenously with anti-HA MAb (1 mg/mouse, given intravenously) on day −0.5, followed by intranasal infection with GAS on day 0. Mouse mortality was observed for 12 days after the GAS infection. #, $P < 0.001$ (compared to ● data).

after further intranasal infection with sublethal doses of GAS strains (Fig. 1 and Table 1). The majority of the superinfected mice died within 4 or 5 days of the GAS infection. The mortality rate of mice superinfected with TSLS-GAS strains was higher than that of mice superinfected with non-TSLS-GAS strains (Table 1). In addition, almost 10% of the dead mice had developed necrotizing fasciitis. It is not easy to elucidate the similarities and differences of influenza virus infection in mice and in humans from the results of the present study because the method used was not the same as infection via the upper respiratory tract in humans. However, since influenza virus infection leads both mice and humans to acute respiratory inflammation, we believe that the pathogenicity of influenza virus infection in mice and humans may be similar.

The most intriguing result from the present mouse model was the appearance of necrotizing fasciitis at the forelimb and hind leg but not the primary infection sites such as the upper respiratory tract and skin (Fig. 3A and Table 2). Mice with necrotizing fasciitis carried greater numbers of GAS organisms in their blood and internal organs compared to those that died without necrotizing fasciitis (Fig. 3E). Furthermore, aggregated clusters of GAS organisms were frequently seen in blood vessels near the affected sites (Fig. 3C). These results suggest that the outbreak of necrotizing fasciitis is induced by GAS that has spread via sepsis from the original infection site.

GAS bacteria were most frequently recovered from the lungs and other organs of dead mice after the superinfection, where IAV coexisted with GAS for up to 24 h after the GAS infection of IAV-infected mice (Fig. 4). Thus, there is the possibility that IAV-infected alveolar epithelial cells that express HA promote the internalization of GAS into these cells (Fig. 5). HA, a 75-kDa protein expressed on the capsule of the virus (26), participates in the fusion between the virus envelopes and endosomes of virus-infected cells prior to viral invasion of the cytoplasm (4, 5, 13). Recently, HA has been shown to bind to sialic acid present in the capsule of group B strep-
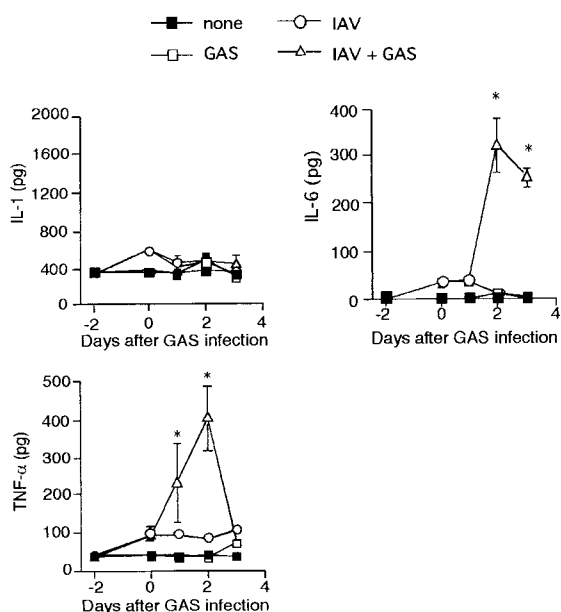
FIG. 8. Production of cytokines in BAL fluid of superinfected, monoinfected, and noninfected mice. Mice were divided into four groups (10 mice per group) as indicated in the figure. BAL fluids from the mice were harvested, and the amounts of IL-1β, IL-6, and TNF-α were measured by enzyme-linked immunosorbent assay. Values are presented as the mean picograms per milliliter of BAL fluid ± the standard deviation. ∗, $P < 0.05$ (compared to IAV [○] and GAS [□]).

tococcus (15). We observed with an electron microscope that IAV also binds to GAS directly (Fig. 5C). Furthermore, we determined the quantitative direct binding of GAS to IAV by counting the GAS organisms bound to IAV coated on the plate. In the experiment, the number of bacteria bound to the plate coated with 4 μg of IAV/ml was 10 times higher than the number of bacteria bound to the plate not coated with IAV (unpublished data). These results suggest that binding of GAS and IAV by HA expression might contribute to the enhanced pathogenicity of invasive GAS infection during dual infection. The organisms of GAS from TSLS and non-TSLS origins were found to possess only trace amounts of sialic acid. Pretreatment of the GAS with sialidase did not affect internalization of the bacterial cells to the IAV-infected epithelial cells (data not shown). Therefore, the ligand to HA remains to be determined.

It should be noted that prior nonlethal IAV infection was critically important for bacteria to accomplish an invasive type of infection in the lungs. In fact, GAS infection prior to IAV infection or simultaneous infection with GAS and IAV did not increase mouse mortality (Fig. 1A). HA was expressed on the alveolar epithelial cells within 24 h after IAV infection (Fig. 6), which then promoted GAS internalization. However, treatment with anti-HA MAb suppressed this internalization and therefore suppressed the outbreak of the invasive GAS infection (Fig. 6 and 7).

Dallaire et al. (7) demonstrated that the induction of severe pneumonia by infection with *Streptococcus pneumoniae* was associated with an increment of proinflammatory cytokine productions. In the present study, we found that the secretion

levels of IL-6 and TNF-α in the BAL fluid of superinfected mice were significantly higher than in the BAL fluid from IAV- or GAS-infected mice (Fig. 8). The highest levels of these cytokines were detected 2 to 3 days after GAS infection. Taken together, an incremental increase of proinflammatory cytokines is followed by an enhanced internalization of GAS in the lungs caused by the superinfection, which results in severe pneumonia.

Several investigators have reported that the expression of SPEA in GAS might be associated with the outbreak of invasive GAS infection (6, 10, 16, 35). In this regard, Zhang et al. (39) found that mice given nonlethal doses of IAV and SEB died within 4 days of the SEB exposure, which suggests that streptococcal superantigen, mitogenic factor, SPEA, and SPEC play important roles in the induction of the lethal synergism. However, no correlation between the expression of the superantigen genes of GAS and mortality in superinfected mice was found in the present study (Table 1). Therefore, superantigens did not significantly affect the pathogenesis of the experimental invasive diseases in mice with superinfection.

In the northern hemisphere, seasonal peaks of infection by both IAV and GAS occur from October to April (3, 28). Indeed, more than 80% of the invasive GAS infection of patients in Canada in 1990 to 1991 were found to occur in winter (8). A recent investigation revealed that more than 90% of those who died from lethal Spanish influenza virus (type A, H1N1) infections exhibited various symptoms of severe bacterial pneumonia (37). The prevalence of GAS-dependent necrotizing fasciitis was also shown in the period when Spanish influenza virus infections prevailed (25, 38). Taken together, these findings suggest that some patients with invasive GAS infection may also be infected with IAV. Therefore, the correlation between the outbreak of disease and the mixed infection requires clarification in humans. In addition, Locci (23) suggested that secondary bacterial infections, e.g., *Staphylococcus aureus*, GAS, group B streptococcus, *Streptococcus pneumoniae*, and *Haemophilus influenzae*, are closely associated with complications in influenza. Some groups of researchers have also found that infection with bacteria after IAV infection leads to the death of mice (11, 14, 17, 22, 24). In the present study, all mice infected with both IAV and GAS developed severe pneumonia (Fig. 2), which we determined to be due to the GAS infection. This fact raises the possibility that HA expressed on the virus-infected alveolar epithelial cells after IAV infection may lead to different kinds of bacterial infections in the lungs.

In the present study, we have established a novel and unique mouse model for the induction of invasive GAS infection in order to mimic human TSLS. The induction of invasive diseases in this model system is mainly due to the existence of IAV HA on the epithelial surfaces of lung tissues. Therefore, it is quite possible that a mixed infection with the influenza virus and GAS is one of the most essential factors causing outbreaks of invasive GAS diseases.

REFERENCES

1. **Ashbaugh, C. D., H. B. Warren, V. J. Carey, and M. R. Wessels.** 1998. Molecular analysis of the role of the group A streptococcal cysteine protease, hyaluronic acid capsule, and M protein in a murine model of human invasive soft-tissue infection. J. Clin. Investig. **102:**550–560.
2. **Baxter, F., and J. McChesney.** 2000. Severe group A streptococcal infection and streptococcal toxic shock syndrome. Can. J. Anaesth. **47:**1129–1140.
3. **Brammer, T. L., H. S. Izurieta, K. Fukuda, L. M. Schmeltz, H. L. Regnery, H. E. Hall, and N. J. Cox.** 2000. Surveillance for influenza—United States, 1994–95, 1995–96, and 1996–97 seasons. Morb. Mortal. Wkly. Rep. CDC Surveill. Summ. **49:**13–28.
4. **Bullough, P. A., F. M. Hughson, J. J. Skehel, and D. C. Wiley.** 1994. Structure of influenza hemagglutinin at the pH of membrane fusion. Nature **371:**37–43.
5. **Chernomordik, L. V., V. A. Frolov, E. Leikina, P. Bronk, and J. Zimmerberg.** 1998. The pathway of membrane fusion catalyzed by influenza hemagglutinin: restriction of lipids, hemifusion, and lipidic fusion pore formation. J. Cell Biol. **140:**1369–1382.
6. **Cunningham, M. W.** 2000. Pathogenesis of group A streptococcal infections. Clin. Microbiol. Rev. **13:**470–511.
7. **Dallaire, F., N. Ouellet, Y. Bergeron, V. Turmel, M.-C. Gauthier, M. Simard, and M. G. Bergeron.** 2001. Microbiological and inflammatory factors associated with the development of pneumococcal pneumonia. J. Infect. Dis. **184:**292–300.
8. **Demers, B., A. E. Simor, H. Vellend, P. M. Schlievert, S. Byrne, F. Jamieson, S. Walmsley, and D. E. Low.** 1993. Severe invasive group A streptococcal infections in Ontario, Canada: 1987–1991. Clin. Infect. Dis. **16:**792–800.
9. **Ehrengut, W., and D. E. Sarateanu.** 1978. A/FM1/47 antibody response in the aged after vaccination with A/New Jersey 76 vaccine. Lancet **i:**440.
10. **Eriksson, B. K., J. Andersson, S. E. Holm, and M. Norgren.** 1998. Epidemiological and clinical aspects of invasive group A streptococcal infections and the streptococcal toxic shock syndrome. Clin. Infect. Dis. **27:**1428–1436.
11. **Gardner, I. D., and T. M. Kung.** 1980. Histopathological changes in the lungs of influenza-induced mice superinfected with *Staphylococcus aureus*. Br. J. Exp. Pathol. **61:**415–420.
12. **Gonzalez-Ruiz, A., G. L. Ridgway, S. L. Cohen, C. P. Hunt, G. McGrouther, and M. Adiseshiah.** 1995. Varicella gangrenosa with toxic shock-like syndrome due to group A *Streptococcus* infection in an adult: case report. Clin. Infect. Dis. **20:**1058–1060.
13. **Hernandez, L. D., L. R. Hoffman, T. G. Wolfsberg, and J. M. White.** 1996. Virus-cell and cell-cell fusion. Annu. Rev. Cell. Dev. Biol. **12:**627–661.
14. **Hernandez, E., F. Ramisse, P. Gros, and J.-D. Cavallo.** 2000. Super-infection by *Bacillus thuringiensis* H34 or 3a3b can lead to death in mice infected with the influenza A virus. FEMS Immunol. Med. Microbiol. **29:**177–181.
15. **Hosaka, Y., A. Ikeura, Y. Harada, K. Kuroda, H. Hamayasu, T. Suzuki, K. Yamada Y. Kawase, and Y. Suzuki.** 2000. Binding of influenza type A viruses to group B *Streptococcus* and haemagglutinination by virus-bound bacteria. J. Electron Microsc. **49:**765–773.
16. **Johnson, D. R., D. L. Stevens, and E. L. Kaplan.** 1992. Epidemiologic analysis of group A streptococcal serotypes associated with severe systemic infections, rheumatic fever, or uncomplicated pharyngitis. J. Infect. Dis. **166:**374–382.
17. **Jones, W. T., J. H. Menna, and D. E. Wennerstrom.** 1983. Lethal synergism induced in mice by influenza type A virus and type Ia group B streptococci. Infect. Immun. **41:**618–623.
18. **Kaul, R., A. McGeer, D. E. Low, K Green, B. Schwartz, et al.** 1997. Population-based surveillance for group A streptococcal necrotizing fasciitis: clinical features, prognostic indications, and microbiologic analysis of seventy-seven cases. Am. J. Med. **103:**18–24.
19. **Kawabata, S., E. Kunitomo, Y. Terao, I. Nakagawa, K. Kikuchi, K. Totsuka, and S. Hamada.** 2001. Systemic and mucosal immunizations with fibronec-tin-binding protein FBP54 induce protective immune responses against *Streptococcus pyogenes* challenge in mice. Infect. Immun. **69:**924–930.
20. **Kawabata, S., H. Kuwata, I. Nakagawa, S. Morimatsu, K. Sano, and S. Hamada.** 1999. Capsular hyaluronic acid of group A streptococci hampers their invasion into human pharyngeal epithelial cells. Microb. Pathog. **27:**71–80.
21. **Layne, S. P., T. J. Beugelsdijk, C. K. Patel, J. K. Taubenberger, N. J. Cox, I. D. Gust, A. J. Hay, M. Tashiro, and D. Lavanchy.** 2001. A global lab against influenza. Science **293:**1729.
22. **LeVine, A. M., V. Koeningknecht, and J. M. Stark.** 2001. Decreased pulmonary clearance of *S. pneumoniae* following influenza A infection in mice. J. Virol. Methods **94:**173–186.
23. **Locci, C. G.** 1973. Influenza and the interaction of viruses and bacteria in respiratory infections. Medicine **52:**369–384.
24. **McCullers, J. A., and J. E. Rehg.** 2002. Lethal synergism between influenza virus and *Streptococcus pneumoniae*: characterization of a mouse model and the role of platelet-activating factor receptor. J. Infect. Dis. **186:**341–350.
25. **Meleney, F. L.** 1924. Hemolytic *Streptococcus* gangrene. Arch. Surg. **9:**317–364.
26. **Melikyan, G. B., S. Lin, M. G. Roth, and F. S. Cohen.** 1999. Amino acid sequence requirements of the transmembrane and cytoplasmic domains of influenza virus hemagglutinin for viable membrane fusion. Mol. Biol. Cell **10:**1821–1836.
27. **Murakami, J., S. Kawabata, Y. Terao, K. Kikuchi, K. Totsuka, A. Tamaru, C. Katsukawa, K. Moriya, I. Nakagawa, I. Morisaki, and S. Hamada.** 2002. Distribution of *emm* genotypes and superantigen genes of *Streptococcus pyogenes* isolated in Japan, 1994–99. Epidemiol. Infect. **128:**397–404.
28. **Musher, D. M., R. J. Hamill, C. E. Wright, J. E. Clarridge, and C. M. Ashton.** 1996. Trends in bacteremic infection due to *Streptococcus pyogenes* (group A *Streptococcus*), 1986–1995. Emerg. Infect. Dis. **2:**54–56.
29. **Nakagawa, I., M. Nakata, S. Kawabata, and S. Hamada.** 2001. Cytochrome *c*-mediated caspase-9 activation triggers apoptosis in *Streptococcus pyogenes* infected epithelial cells. Cell. Microbiol. **3:**395–405.
30. **Nakashima, K., S. Ichiyama, Y. Iinuma, Y. Hasegawa, M. Ohta, K. Ooe, Y. Shimizu, H. Igarashi, T. Murai, and K. Shimokata.** 1997. A clinical and bacteriologic investigation of invasive streptococcal infections in Japan on the basis of serotypes, toxin production, and genomic DNA fingerprints. Clin. Infect. Dis. **25:**260–266.
31. **Okamoto, S., S. Kawabata, I. Nakagawa, and S. Hamada.** 2001. Administration of superantigens protects mice from lethal *Listeria monocytogenes* infection by enhancing cytotoxic T cells. Infect. Immun. **69:**6633–6642.
32. **Okuno, Y., Y. Isegawa, F. Sasao, and S. Ueda.** 1993. A common neutralizing epitope conserved between the hemagglutinins of influenza A virus H1 and H2 strains. J. Virol. **67:**2552–2558.
33. **Okuno, Y., K. Tanaka, K. Baba, A. Maeda, N. Kunita, and S. Ueda.** 1990. Rapid focus reduction neutralization test of influenza A and B viruses in microtiter system. J. Clin. Microbiol. **28:**1308–1313.
34. **Reid, S. D., N. P. Hoe, L. M. Smoot, and J. M. Musser.** 2001. Group A *Streptococcus*: allelic variation, population genetics, and host-pathogen interactions. J. Clin. Investig. **107:**393–399.
35. **Stevens, D. L., M. H. Tanner, J. Winship, R. Swarts, K. M. Ries, P. M. Schlievert, and E. Kaplan.** 1989. Severe group A streptococcal infections associated with a toxic shock-like syndrome and scarlet fever toxin A. N. Engl. J. Med. **321:**1–7.
36. **Svensson, N., S. Oberg, B. Henriques, S. Holm, G. Kallenius, V. Romanus, and J. Giesecke.** 2000. Invasive group A streptococcal infections in Sweden in 1994 and 1995: epidemiology and clinical spectrum. Scand. J. Infect. Dis. **32:**609–614.
37. **Taubenberger, J. K., A. H. Reid, and T. G. Fanning.** 2000. The 1918 influenza virus: a killer comes into view. Virology **274:**241–245.
38. **Weiss, S. A.** 1997. Group A *Streptococcus* invasive infections: a review. Can. J. Surg. **40:**18–25.
39. **Zhang, W. J., S. Sarawar, P. Nguyen, K. Daly, J. Rehg, P. C. Doherty, D. L. Woodland, and M. A. Blackman.** 1996. Lethal synergism between influenza infection and staphylococcal enterotoxin B in mice. J. Immunol. **157:**5049–5060.